Biophysical Journal Volume 71 September 1996 1422–1427

Preferential Partitioning of Melittin into the Air/Water Interface: Structural and Thermodynamic Implications

Gerhard Wackerbauer, Ingrid Weis, and Gerhard Schwarz
Department of Biophysical Chemistry, Biocenter of the University of Basel, Basel, Switzerland

ABSTRACT The membrane active agent melittin has been investigated with regard to the formation of a Langmuir monolayer and the accordingly induced surface activities. We show that in spite of its considerable solubility in an aqueous medium, this peptide nevertheless largely accumulates in the air/water interface unless the lateral pressure is raised beyond a certain threshold value depending on the pH in the subphase. The true surface concentrations have been determined by means of a recently developed novel method based on thermodynamic principles. It affords an access to the partitioning equilibrium between the surface and subphase domains, provided the latter surrounding is not excessively preferred. In the present case this approach was used to derive quantitative information on the pertinent interfacial structure and thermodynamics. In particular, the apparent molecular area and the Gibbs energy of mutual interaction in the monolayer could be evaluated as a function of the applied surface pressure. The data suggest the existence of two structural conversions in the course of an increasing lateral compression. The surface-associated peptide accordingly assumes three different states of successively reduced area requirements, supposedly owing to an orientational transition involving a straightening up of a helical conformation. This conclusion is corroborated by surface potential measurements reflecting corresponding changes of the effective dipole moment perpendicular to the surface.

INTRODUCTION

There is a multitude of small peptides (comprising some 10 to 40 amino acid residues) that exhibit a pronounced potential to control functional properties of biological membranes. This includes translocation, pore formation, fusion, and signal transduction processes. Amphipathic primary structures where, in an α-helical conformation, hydrophobic and hydrophilic faces emerge have attracted special interest. They are thought to be a basic element of a membrane channel protein (Ojcius and Young, 1991). Accordingly, amphipathic peptides have become popular models of pore formers in lipid bilayers (Sansom, 1991). Among this category falls melittin (26 residues), the main constituent of bee venom, whose actions on membranes have been studied in especially great detail (Dempsey, 1990). A fundamental issue in this context concerns the partitioning of the peptide between liposomal membranes and their aqueous surroundings (Schwarz and Beschiaschvili, 1989; Schwarz, 1996). Useful quantitative information about relevant lipid-peptide interactions in structural and thermodynamic terms may also be derived from data obtained with experiments on Langmuir monolayers at the hydrophobic/hydrophilic phase boundary of an air/water interface.

Because of their hydrophobic properties, membrane-active peptides can generally be expected to exhibit surface activity. In particular, a number of pertinent studies can be found in the literature regarding the gramicidins (Davian-Van Mau et al., 1987; Dhathathreyan et al., 1988; Tournois et al., 1989). Following conventional usage, the observed surface pressure is plotted versus the average area per molecule based on the total amount of peptide added to the system. This would be a reasonable approach, provided one deals with an insoluble monolayer (Gaines, 1966). Actually, however, it appears unclear whether some of the spread peptide was lost in the subphase, so that the true molecular area in the interface becomes larger than expected. Because such an effect should depend on the surface pressure and the area/volume ratio of the system (Schwarz et al., 1996), it could possibly result in a faulty course of the conventionally evaluated pressure-area isotherm. In any event, melittin has also been investigated in an analogous manner, assuming negligible accumulation in the aqueous subphase (Birdi et al., 1983; Gevod and Birdi, 1984; Birdi and Gevod, 1987). The latter surmise is especially remarkable in view of the high solubility in water that has been established for this peptide. In the present article we present a more advanced study based on a novel approach to analyzing Langmuir monolayer experiments (Schwarz and Taylor, 1995). It offers a definite means of determining the extent of partitioning between a monomolecular film at the air/water interface and its aqueous subphase, provided the amount of surfactant in the bulk volume remains reasonably small. This method is quite generally applicable. In the present work we have applied it to the case of small amounts of melittin spread on the surface of a Langmuir trough. The data clearly reveal that appreciable desorption may indeed set in only at fairly high surface pressures (depending on pH) where the peptide molecules are apparently squeezed together at a distance of rather strong repulsion. The results are discussed quantitatively in terms of the related structural and thermodynamic properties. This includes the partitioning equilibrium as

Received for publication 27 February 1996 and in final form 17 May 1996.

Address reprint requests to Dr. Gerhard Schwarz, Department of Biophysical Chemistry, Biocenter of the University, Klingelbergstrasse 70, CH 4056 Basel, Switzerland. Tel.: +41-61-267-2200; Fax: +41-61-267-2189; E-mail: weis@ubaclu.unibas.ch.

0006-3495/96/09/1422/06 $2.00

well as the Gibbs energy of interaction and two apparently orientational transitions of the interfacial peptide.

MATERIALS and METHODS

Chemicals

For the aqueous solutions we always used quartz glass distilled and deionized water produced with a NANOpure apparatus (Barnstead Thermolysine Co., Dubuque, IA). The McIlvain buffer was always freshly prepared from dry citric acid monohydrate and disodium phosphate dihydrate (p.a. quality; Fluka Chemie AG, Buchs, Switzerland). It had an ionic strength of 60 mM.

Melittin prepared from bee venom was supplied by Mack Chemical Co. (Illertissen, Germany). We have purified it via high-performance liquid chromatography to remove phospholipase A_2. The employed aqueous stock solution was checked for pureness by means of high-performance capillary electrophoresis, during which it showed a single sharp line. Its concentration has been determined with optical absorption measurements (Quay and Condie, 1983). It was then stored in small amounts at −20°C.

Monolayer experiments

Basically we have employed the same technical procedures described previously in more detail (Schwarz and Taylor, 1995). Pressure versus trough area isotherms involving a fixed amount of spread peptide were recorded upon a comparably slow compression of the monolayer (5 cm^2/min) in a Fromherz trough (Fromherz, 1975) with a Wilhelmy platelet (Gaines, 1966). In addition, the "isochorous mode" of measurement has been applied, i.e., the equilibrium surface pressure that was eventually established was registered with a greater and greater total amount of substance at various fixed areas (employing a set of several troughs with equal volume, but different air/water interfacial areas). The results of both methods agreed quite well, so that equilibrium can be considered to exist also for the isotherms (see Results and Fig. 1).

The peptide was always added with a calibrated injection microsyringe (Hamilton Co., Reno, NV) from the stock solution. It was carefully deposited as a drop on the surface (starting at a maximum trough area when measuring the isotherms). The total amount of peptide was calculated from the added volume and the concentration of the stock solution. The subphase was stirred with a magnetic stirrer. All measurements were done at room temperature (23 ± 1°C) and atmospheric pressure.

Spreading the melittin onto the interface has the advantage of a comparatively large concentration gradient in the unstirred diffusion layer. This ensures a reasonably fast equilibration of the partitioning process. The reverse procedure proved to be less useful. When we injected the same small amounts of peptide (a few nanomoles) into the subphase, the lateral pressure increased much too slowly. Presumably the driving force is substantially reduced, owing to the rather small relevant concentration gradient. Indeed, the pressure developed quite rapidly up to the value measured with spread material upon the injection of sufficiently large amounts of peptide, which were, however, beyond those of interest here.

The true surface concentration, Γ, of interfacial melittin could be determined by applying a method introduced in the case of a poorly soluble peptide (Schwarz and Taylor, 1995). This implies surface activity measurements with a series of experiments involving different amounts of total surfactant, n_o, as initially spread on a Langmuir trough. Then we plot the various n_o versus the appropriate area of the monolayer, A, taken at constant surface pressure, π. Because of mass conservation the relation

$$n_o = \Gamma \cdot A + n_s \tag{1}$$

must hold with n_s standing for the amount of surfactant in the aqueous subphase. Under the circumstances of fixed surface pressure and bulk volume (V = 48 ml), the quantities Γ as well as n_s remain invariant, so that the plot of n_o versus A is predicted to become a straight line, the slope of which would be equal to the surface concentration at the given surface pressure, whereas the intercept on the ordinate axis turns out to be the amount of surfactant that seeped away into the bulk volume. Such an approach should be very generally applicable, provided n_s remains sufficiently smaller than n_o. In particular, one may in this way check a so-called insoluble monolayer to determine how much of the material that was initially spread on the surface was lost by desorption. A pertinent study carried out with the membrane lipid palmitoyloleoylphosphatidylcholine actually revealed that in contrast to a widely held view, substantial desorption of the monolayer may occur (Schwarz et al., 1996). It would be generally difficult to determine the small subphase concentrations otherwise. In the present case, a fairly reliable measurement of the Trp fluorescence signal was only possible above at least 70 nM, which is outside the range of preferential partitioning under consideration.

For the surface potential measurements the Kelvin vibrating plate method was used (Gaines, 1966). A voltage was supplied on a periodically changing capacitor consisting of a Ag/AgCl electrode in the subphase and a vibrating flat gold electrode (diameter ≈ 2 cm) about 1 mm above the monolayer, so that the potential drop, ΔV_m, across the monolayer is compensated. A more detailed description of the experimental set-up has been given elsewhere (Winterhalter et al., 1995).

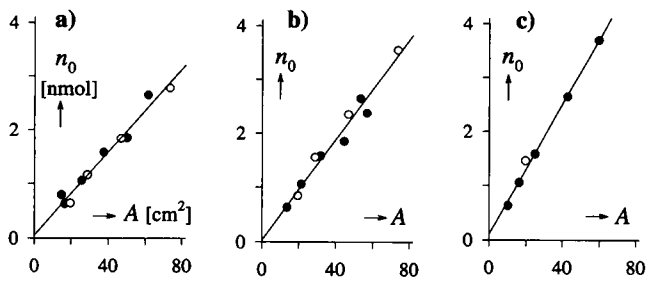

FIGURE 1 Total amount of melittin versus the area of the monolayer (at pH 7 in the subphase) for the three fixed surface pressures 10 mN/m (*a*), 20 mN/m (*b*), and 30 mN/m (*c*), respectively. ●, Data from isotherms; ○, data taken from isochors (see text).

RESULTS

Fig. 1 shows specimen plots of total amounts of melittin versus the area of the monolayer, subject to a fixed surface pressure at a pH of 7.0 (± 0.1) in the subphase. This includes data from both isotherms and isochors. They agree quite satisfactorily, indicating that equilibrium was actually established during the measurement of the isotherms. In these cases and analogous ones for other surface pressures, sufficiently pronounced straight lines are observed as predicted by Eq. 1. Subsequently, the surface concentration, Γ (slope), and the amount of peptide in the subphase, n_s (intercept on the ordinate axis), have been evaluated. The characteristic quantities of the partitioning equilibrium, namely Γ and the subphase concentration $c_s = n_s/V$, respectively, are presented in Fig. 2 as a function of the applied lateral pressure.

It turned out that changing the pH in the subphase had an effect on the quantitative features of the phenomenon under consideration. This is demonstrated by the partitioning data shown in Fig. 3 for a somewhat enhanced pH of 7.9 (± 0.1).

Furthermore, the surface potential ΔV_m has been measured under equivalent conditions. It can be related to the surface concentration as pointed out in the Appendix. We

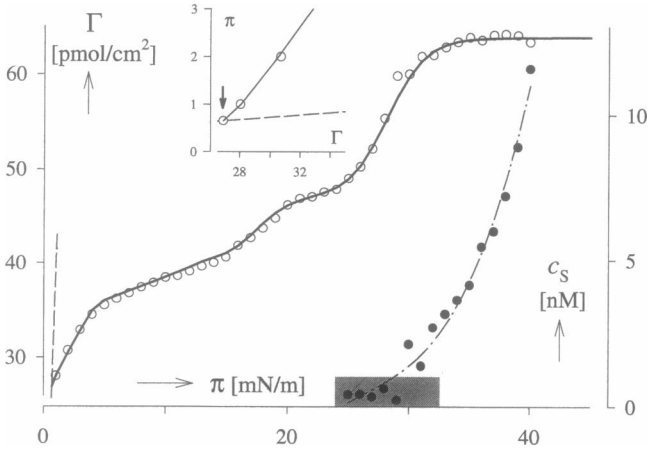

FIGURE 2 True surface concentrations (○) and molarities of melittin desorbed in the subphase (●) evaluated (at pH 7) from linear plots according to those shown in Fig. 1. The shaded stripe (with $c_s \leq 1$ nM) stands for the approximate error bar of the subphase concentration. The inset blows up the range of low surface pressure where the "ideal" course (dashed line) is supposed to merge with extrapolated data points at Γ_o (indicated by the arrow). This is supposed to imply the onset of substantial peptide-peptide interactions (see text).

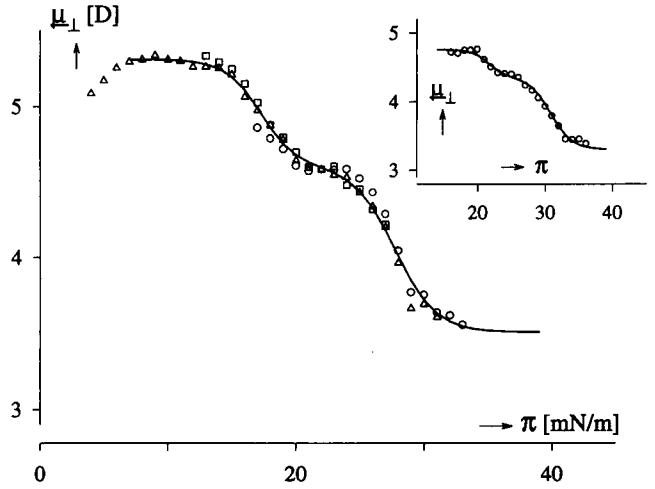

FIGURE 4 Normal component (positive toward air) of the effective interfacial dipole moment per molecule (in Debye units) at pH 7. This comprises results from three independent runs of surface potential measurements (indicated by different symbols), the absolute level of which has been averaged to correct for zero-point drifts. The analogous results and curve fit for pH 7.9 are presented in the inset (with plateau values 4.8 D, 4.4 D, and 3.3 D, respectively). The appropriate absolute level is, however, affected by a higher uncertainty (~5% according to the given error bar), because only a single run of measurements has been carried out.

have accordingly evaluated an effective molecular dipole moment normal to the interface:

$$\underline{\mu}_\perp = \underline{\mu}^\circ_\perp / \epsilon = \epsilon_o \cdot a_p \cdot \Delta V_m, \qquad (2)$$

where ϵ_o is the permittivity of vacuum; ϵ is the relative dielectric constant in the monolayer; and $\underline{\mu}^\circ_\perp$ is the true dipole moment. This structural property is found to exhibit a well-characterized dependence on the applied surface pressure, as illustrated by Fig. 4. It should be noted that the measured value of ΔV_m is subject to a possible uncertainty of up to 5%, owing to a slow zero-point drift (which may be reduced by averaging the results of several runs). At any rate, the relative error in a single run is only about 0.5%, ensuring a quite precise reproducibility of positions and amplitudes exhibited by the apparent steps of $\underline{\mu}_\perp$ upon monolayer compression.

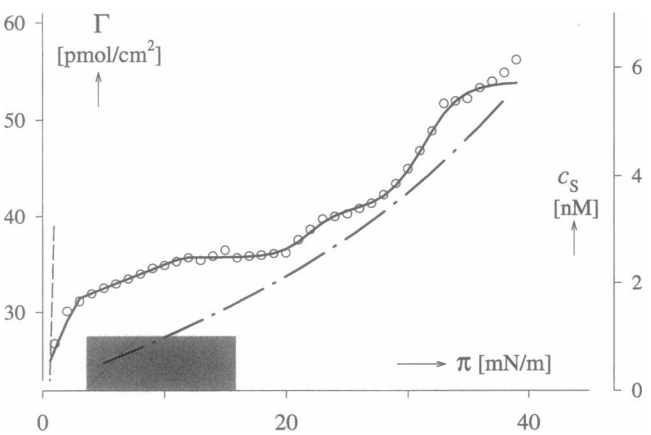

FIGURE 3 Surface concentrations (○) at pH 7.9. The subphase concentrations are displayed by the dashed-dotted curve (no individual data points shown, for clarity).

DISCUSSION

The experimental evidence for pH 7 compiled in Fig. 2 clearly manifests a very strong preference of the melittin molecules for an accumulation in the air/water interface. Apparently it is the excessive mutual repulsion eventually being encountered at lateral pressures higher than about 30 mN/m that limits the actual surface concentration to some 64 pmol/cm^2 and drives additional peptide into the subphase. The actual extent of desorption may be illustrated by a practical example. Let us consider a subphase concentration of only 2 nM, as observed at about 31 mN/m (where $\Gamma \approx 62$ pmol/cm^2). This would imply $n_s = Vc_s \approx 0.1$ nmol. In the case of a surface area of 20 cm^2, the total amount originally spread was $n \approx 1.34$ nmol according to Eq. 1. Then 7.5% of it must have been desorbed in the aqueous bulk domain. Increasing the pH apparently favors partitioning into the subphase to an appreciable degree, as demonstrated by the results presented in Fig. 3 for pH 7.9. Appreciable desorption is encountered already at some 10 mN/m. There is, however, a less steep increase upon the applied pressure.

Because we have determined the true surface concentration, we may convert it to the actual molecular area, $a_p = 1/N_A\Gamma$ (where N_A is Avogadro's number), i.e., the average area available per molecule in the interface. How this rather expressive feature is changed upon monolayer compression has been displayed in Fig. 5.

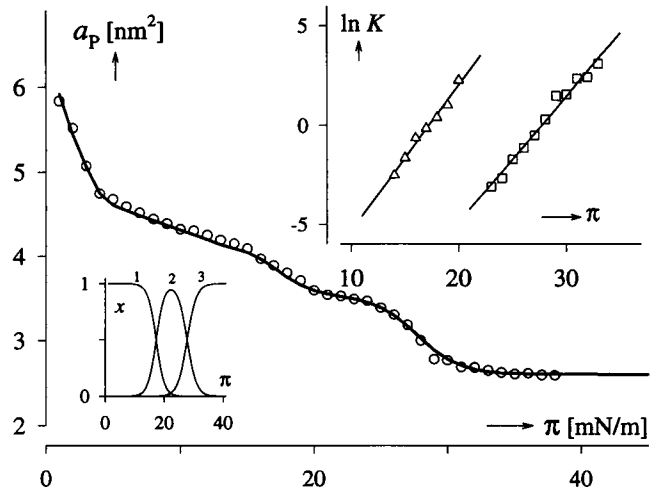

FIGURE 5 Change in the area per molecule in the interface upon compression of the monolayer (at pH 7). The inset at the upper right demonstrates the existence of van't Hoff relations reflecting two interfacial transitions (see text). The respective molar fractions of the three proposed states are shown in the inset at the lower left.

A quantitative approach to the underlying structural and thermodynamic properties may be based on an analysis of ΔG_m, i.e., the Gibbs energy of peptide-peptide interaction per mole in the monolayer. We shall do this along the lines described previously in greater detail (Schwarz and Taylor, 1995). A brief review is given below in the Appendix.

The magnitude of ΔG_m can be calculated as a function of Γ in terms of an appropriate activity coefficient α as

$$\Delta G_m/RT = \ln \alpha = \varphi + \int_0^{\Gamma} (\varphi/\Gamma) \cdot d\Gamma \tag{3}$$

where $\varphi = (\pi/\pi_{id}) - 1,$

with $\pi_{id} = RT \cdot \Gamma$. In the "ideal" case (no peptide-peptide interactions) one has $\varphi = 0$ ($\alpha = 1$). According to the data in Fig. 2 this will be applicable below $\Gamma_o = 26.9$ pmol/cm^2 (being equivalent to $\pi_o = 0.66$ mN/m, $a_o = 6.17$ nm^2, $\Delta G_m = 0$). The course of ln α calculated in this way with the experimental values of φ for $\Gamma > \Gamma_o$ is presented in Fig. 6.

Because of the increased crowding of the molecules upon compression of the monolayer, one would expect a continuous upward bending of the ln α versus Γ curve with a tendency to approach infinity at a state of densest packing. We note, however, a definite relief of the apparent repulsion forces above a characteristic surface concentration Γ_1 with two further turning points at Γ_2 and Γ_3 further beyond (see Table 1 for the numerical details).

We propose to interpret these features in terms of the specific molecular interactions taking place in four consecutive ranges of Γ and π, respectively. The appropriate quantitative model has been used to calculate the solid fit curves in our diverse figures.

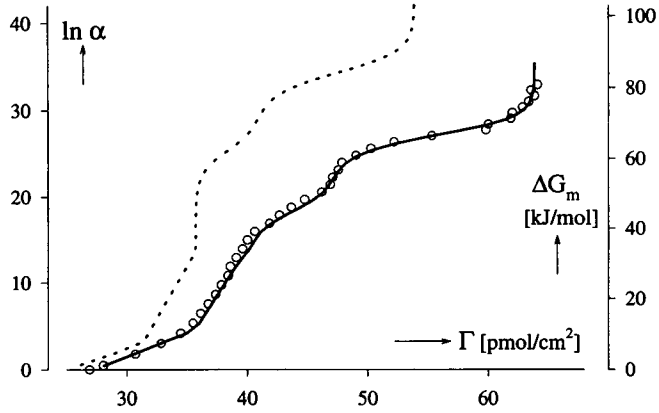

FIGURE 6 Logarithm of the apparent activity coefficient (left scale) and the Gibbs energy of peptide-peptide interaction in the monolayer (right scale), respectively, at pH 7, calculated from the experimental data by means of Eq. 3. The dashed curve represents the result obtained for pH 7.9.

Range 1 ($\Gamma_o < \Gamma < \Gamma_1$) is presumed to comprise a compression of the monolayer involving only molecules in an initial state 1 with an excluded self-area $a_1 = 1/N_A\Gamma_1$. At the end of this range a_p has eventually dropped to a_1. In Fig. 6 we observe a transition between two practically linear relationships of ΔG_m. First we have

$$\ln \alpha = 2b_o \cdot (\Gamma - \Gamma_o), \tag{4a}$$

holding true up to $\Gamma_\bullet$. By application of Eqs. A1a, A1b, and A2, this may be converted to a fit function for the surface pressure expressed as

$$\pi = RT \cdot [\Gamma + b_o \cdot (\Gamma^2 - \Gamma_2^o)]. \tag{4b}$$

At $\Gamma_\bullet$ another linear relation with a substantially enhanced slope becomes effective, namely,

$$\ln \alpha = 2b_\bullet \cdot (\Gamma - \Gamma'_\bullet), \tag{5a}$$

TABLE 1 Numerical details of the characteristic ranges of monolayer compression (see text) for a pH of 7.0 (±0.1) in the subphase

	pmol/cm^2	a_p (nm^2)	π (mN/m)	ln α	ΔG_m (kJ/mol)
a) Bounding surface concentrations with pertinent values of other relevant structural and thermodynamic quantities					
Γ_o	26.9 (24.9)	6.17 (6.67)	0.66 (0.61)	0	0
$\Gamma_\bullet$	35.7 (31.3)	4.65 (5.31)	4.35 (2.8)	4.5 (3.5)	11.1 (8.6)
Γ_1	39.6 (36.3)	4.20 (4.58)	13.0 (12.8)	13.8 (17.2)	33.8 (42.2)
Γ_2	47.1 (40.7)	3.53 (4.08)	22.0 (25.8)	22.2 (29.2)	54.4 (71.6)
Γ_3	63.9 (55.0)	2.60 (3.02)	36.0 (38.1)	32.0 (39.5)	78.4 (96.8)

b) Parameters of the eqs. 4a, 5a
$b_o = 0.26$ (0.23) cm^2/pmol
$b_\bullet = 1.10$ (1.19) cm^2/pmol, $\Gamma'_\bullet = 34.0$ (30.8) pmol/cm^2

c) Parameters of the eqs. 6a, b
$\underline{k}_1 = 0.73$ (0.83) m/mN, $\underline{\pi}_1 = 17.2$ (21.7) mN/m
$\underline{k}_2 = 0.63$ (0.63) m/mN, $\underline{\pi} = 27.7$ (31.4) mN/m

The respective numbers at pH 7.9 (±0.1) are added in parentheses.

which leads to the appropriate fit function

$$\pi = \pi_{\bullet} + RT \cdot [(\Gamma - \Gamma_{\bullet}) + b_{\bullet} \cdot (\Gamma^2 - \Gamma_{\bullet}^2)], \quad (5b)$$

that applies up to Γ_1. Then we enter a different domain.

Range 2 ($\Gamma_1 < \Gamma < \Gamma_2$) affords conditions that permit the peptide molecules in interfacial state 1 to evade further squeezing by undergoing a transition into state 2 with a lower self-area $a_2 = 1/N_A\Gamma_2$. The a_p will then decrease essentially in proportion to the degree of conversion. Thus the molar fraction of molecules in state 2 becomes

$$x_2 = (a_1 - a_p)/(a_p - a_2).$$

The apparent equilibrium constant $K_1 = x_2/x_1$ ($x_1 = 1 - x_2$) proves to depend on the surface pressure according to a van't Hoff relation

$$\ln K_1 = \underline{k}_1 \cdot (\pi - \underline{\pi}_1) \quad (6a)$$

Such a linearity of $\ln K_1$ versus π is actually demonstrated by our data, as shown in Fig. 5. We suggest that a practically complete turnover into state 2 is accomplished at the end of the present range but is then followed by a second transition.

Range 3 ($\Gamma_2 < \Gamma < \Gamma_3$) indeed reveals another van't Hoff relation for $K_2 = x_3/x_2$:

$$\ln K_2 = \underline{k}_2 \cdot (\pi - \underline{\pi}_2) \quad (6b)$$

(see Fig. 5). This suggests a conversion into an interfacial state 3, the self-area of which is $a_3 = 1/N_A\Gamma_3$.

Within the ranges 2 and 3 the molecular area can now be fairly well described by the incompressibility relation

$$a_p = x_1 \cdot a_1 + x_2 \cdot a_2 + x_3 \cdot a_3 \quad (7)$$

with $x_1 = 1/(1 + K_1 + K_1 \cdot K_2)$, $x_2 = K_1 \cdot x_1$, $x_3 = K_1 \cdot K_2 \cdot x_1$. This implies a fit function for Γ versus π. Once (eventually) $x_3 \rightarrow 1$ at the end of range 3, the interfacial peptide apparently approaches an upper bound of closest packing in a state of self-area a_3 at Γ_3, so that further material will be largely forced away into the subphase.

Range 4 ($\Gamma > \Gamma_3$) thus only allows a minor increase in the surface concentration if still higher lateral pressures are applied.

The self-area of state 1 is about equal to the longitudinal cross section of a cylinder approximating a melittin monomer in its α-helical conformation. Therefore we propose that the molecules assume an initially parallel position in the interface with their hydrophobic faces directed off the water reach. Once the packing becomes too close, straightening-up processes toward states that require less self-area appear to permit more crowding at less expense of free energy.

The present model is very well supported by the effective molecular dipole moments derived from our surface potential data as presented in Fig. 4. They evidently show concurring features of structural transitions at consistent turning points. There are indeed two well-pronounced transitions with nice plateau values $\mu_\perp^{(1)} = 5.3$ D, $\mu_\perp^{(2)} = 4.6$ D, $\mu_\perp^{(3)} = 3.5$ D (Debye units), which are attributed to the proposed interfacial states. The data points can be very well fitted using the same K_1, K_2 (see Eqs. 6a and 6b and Table 1c) for the quantitative description of interfacial transitions employed before with the molecular area:

$$\underline{\mu}_\perp = x_1 \cdot \underline{\mu}_\perp^{(1)} + x_2 \cdot \underline{\mu}_\perp^{(2)} + x_3 \cdot \underline{\mu}_\perp^{(3)}. \quad (8)$$

These features are seen to be reflections of the above-indicated orientational changes brought about by a tilt of a more or less rigid molecule. We note that the effective dielectric constant ϵ in the interface undergoes a dramatic variation between 1 (air) and about 80 (water), so that even small displacements toward the water domain may result in a substantial drop in the observed surface potential.

Finally, it should be emphasized that the fairly moderate rise in the pH has apparently not affected the general qualitative picture of the interfacial equation of state. There are, however, rather remarkable quantitative changes, as exhibited in Table 1 and the diverse figures. Generally we observe an increase in both the individual self-areas and Gibbs energies of interaction.

APPENDIX

Monolayer thermodynamics

We give a brief review of the fundamentals that are relevant in the context of this article. A more detailed account has been outlined previously by Schwarz and Taylor (1995).

To start a quantitative discussion, the chemical potential, μ, of the surfactant solute in its interfacial state must be introduced. Along the lines of conventional treatment it may be formulated as

$$\mu = \mu^{\infty} + RT \cdot \ln \Gamma + \Delta G_m. \quad (A1a)$$

The first two terms represent the "ideal" part applicable to sufficiently high dilution ($\Gamma \rightarrow 0$) where solute-solute interaction does not occur. The standard potential μ^{∞} is determined by the Gibbs energy of solvation (and depends on the special choice for the surface concentration unit), and the logarithmic term allows for the entropy of ideal mixing. Nonideal contributions through mutual interactions when the mole number of surfactant, n, is increased in the interface at constant area are to be taken together in a third term that is also a sole function of Γ, namely,

$$\Delta G_m = (\partial G/\partial n)_A = RT \cdot \ln \alpha, \quad (A1b)$$

so defining an appropriate activity coefficient α (with $\alpha \rightarrow 1$ at $\Gamma \rightarrow 0$).

By integration of Gibbs equation

$$d\pi = \Gamma \cdot d\mu, \quad (A2)$$

one can then readily calculate ΔG_m from experimental π versus Γ data as expressed by Eq. 3. It stands to reason that ΔG_m and $\ln \alpha$, respectively, will steeply grow beyond all limits if the available area per molecule, a_p, approaches the finally incompressible self-area a_1 of the given interfacial state.

An increase in the surface concentrations beyond Γ_1 can only take place once the initial structural state 1 is possibly converted to an alternative state 2 and then perhaps to another state 3 with self-areas $a_3 < a_2 < a_1$. In these cases $\mu_1^{\infty} \ll \mu_2^{\infty} \ll \mu_3^{\infty}$, so that the states requiring less area would eventually come into existence at higher lateral pressures because their activity coefficients increase at a slower rate.

Surface potential

The structural organization of the surfactant and water molecules in the air/water interface may give rise to appreciable dipole moments in the perpendicular direction. This implies an inherent drop in voltage ΔV_m that can easily be related to the total dipolar charge Q by modeling the monolayer as a planar capacitor (with a capacitance $C = \epsilon_o\epsilon \cdot A/d$). Accordingly, we find that the surface potential can be expressed as

$$\Delta V_m = Q/C = ((Q \cdot d)/A)/\epsilon_o\epsilon, \quad \text{(A3)}$$

where ϵ_o is the absolute permittivity of vacuum, ϵ is the effective dielectric constant, and d is the distance of the dipolar charges. Because $Q \cdot d$ is the total dipole moment normal to the surface, we may then divide the surface potential by the surface concentration, resulting in

$$\Delta V_m/\Gamma = N_A \cdot \mu_\perp^o/\epsilon_o\epsilon, \quad \text{(A4)}$$

where $\mu_\perp^o$ denotes the normal component of the true dipole moment per molecule. This can be readily converted to Eq. 2, introduced before in the Results.

We are grateful to Professor R. Benz (Department of Biotechnology, University of, Würzburg, Germany), who kindly made available to us his surface potential apparatus, and to Dr. M. Winterhalter for his valuable advice to do the appropriate measurements.

This work has been supported by grants 31-32188.91 and 31-42045.94 of the Swiss National Science Foundation.

REFERENCES

Birdi, K. S., and V. S. Gevod. 1987. Melittin and ionic surfactant interactions in monomolecular films. *Colloid Polym. Sci.* 265:257–261.

Birdi, K. S., V. S. Gevod, O. S. Ksenzhek, E. Stenby, and K. L. Rasmussen. 1983. Equation of state for monomolecular films of melittin at air-water interface. *Colloid Polym. Sci.* 261:767–775.

Davian-Van Mau, N., B. Daumas, D. Lelièvre, Y. Trudelle, and F. Heitz. 1987. Linear gramicidins at the air-water interface. *Biophys. J.* 51: 843–845.

Dempsey, C. E. 1990. The action of melittin on membranes. *Biochim. Biophys. Acta.* 1031:143–161.

Dhathathreyan, A., U. Baumann, A. Müller, and D. Möbius. 1988. Characterization of complex gramicidin monolayers by light reflection and Fourier transform infrared spectroscopy. *Biochim. Biophys. Acta.* 944: 265–272.

Fromherz, P. 1975. Instrumentation for handling monomolecular films at an air-water interface. *Rev. Sci. Instrum.* 46:1380–1386.

Gaines, G. L., Jr. 1966. Insoluble Monolayers at Liquid-Gas Interfaces. Interscience Publishers, New York.

Gevod, V. S., and K. S. Birdi. 1984. Melittin and the 8–28 fragment. *Biophys. J.* 45:1079–1083.

Ojcius, D. M., and J. D. E. Young. 1991. Cytolytic pore-forming proteins and peptides: is there a common structural motiv? *Trends Biochem. Sci.* 16:225–229.

Quay, S. C., and C. C. Condie. 1983. Conformational studies of aqueous melittin: thermodynamic parameters of the monomer-tetramer self-association reaction. *Biochemistry.* 22:695–700.

Sansom, M. S. P. 1991. The biophysics of peptide models of ion channels. *Prog. Biophys. Mol. Biol.* 55:139–235.

Schwarz, G. 1996. Electrical interactions of membrane active peptides at lipid/water interfaces. *Biophys. Chem.* 58:67–73.

Schwarz, G., and G. Beschiaschvili. 1989. Thermodynamic and kinetic studies on the association of melittin with a phospholipid bilayer. *Biochim. Biophys. Acta.* 979:82–90.

Schwarz, G., and S. E. Taylor. 1995. Thermodynamic analysis of the surface activity exhibited by a largely hydrophobic peptide. *Langmuir.* 11:4341–4346.

Schwarz, G., G. Wackerbauer, and S. E. Taylor. 1996. Partitioning of a nearly insoluble monolayer into its aqueous subphase. *Colloids Surfaces A.* In press.

Tournois, H., P. Gieles, R. Demel, J. de Gier, and B. de Kruiff. 1989. Interfacial properties of gramicidin and gramicidin-lipid mixtures measured with static and dynamic monolayer techniques. *Biophys. J.* 55: 557–569.

Winterhalter, M., H. Bürner, S. Marzinka, R. Benz, and J. J. Kasianowicz. 1995. Interaction of poly(ethylene-glycols) with air-water interfaces and lipid monolayers: investigations on surface pressure and surface potential. *Biophys. J.* 69:1372–1381.